

Received February 13, 2019, accepted February 21, 2019, date of publication February 25, 2019, date of current version March 13, 2019.

Digital Object Identifier 10.1109/ACCESS.2019.2901526

Performance Investigation of DFT-Spread OFDM Signal for Short Reach Communication Systems Beyond NG-PON2

YUPENG LI¹, JIAWEI HAN², AND XIAONAN ZHAO¹

Tianjin Key Laboratory of Wireless Mobile Communications and Power Transmission, Tianjin Normal University, Tianjin 300387, China
College of Electronic and Communication Engineering, Tianjin Normal University, Tianjin 300387, China

Corresponding author: Yupeng Li (fx_lyp@163.com)

This work was supported in part by the Natural Science Foundation of Tianjin under Grant 18JCQNJC70900, Grant 18JCQNJC01900, and Grant 18JCYBJC86400, in part by the Natural Science Foundation of China under Grant 61805176, in part by the Open Fund of the State Key Laboratory of Information Photonics and Optical Communications through the Beijing University of Posts and Telecommunications under Grant IPOC2017B002, and in part by the Doctor Fund of Tianjin Normal University under Grant 52XB1604.

ABSTRACT In this paper, we investigate the performance of a discrete Fourier transform (DFT)-spread OFDM signal in an intensity-modulation/direct-detection system. We find that DFT-spread OFDM could reduce the peak-to-average power ratio effectively and hence improve the nonlinearity tolerance. Furthermore, DFT-spread OFDM also improves the receiver sensitivity performance and shows good robustness to nonlinearity distortion caused by low-bit resolution digital-to-analog converters and analog-to-digital converters. The measured bit error ratio of DFT-spread OFDM signal after a 40-km standard single mode fiber is well less than the forward-error correction limit of 3.8×10^{-3} .

INDEX TERMS DFT-spread, OFDM, PAPR, NG-PON2.

I. INTRODUCTION

To meet the explosive growing bandwidth requirements of services such as internet of things (IOT), high-definition television (HDTV), and mobile fronthaul networks (MFN) of the fifth generation (5G) communication system, massive efforts have been made to improve the capacity of short reach optical communication systems [1]–[3]. Moreover, the passive optical network (PON) [4]–[6] has been widely adopted as one of the main fiber-to-the-home (FTTH) solutions to meet the low-cost demands of the access networks. PON technologies are expected to deliver an aggregate capacity of 40Gb/s and the next generation PON stage 2 (NG-PON2) standardization work has adopted time-/wavelength-division multiplexing (TWDM) scheme to address this problem [7]. However, NG-PON2 still maintains the use of conventional on-off keying (OOK) modulation with transmission speeds preserved at 10Gb/s per wavelength, resulting in a low spectral efficiency (SE). It is widely accepted that the future generation PON technologies must exceed the 10Gb/s per wavelength limitation to further increase access network capacity, and the conventional binary OOK is obviously not an appropriate choice.

The associate editor coordinating the review of this manuscript and approving it for publication was Qilian Liang.

It is preferred to use advanced modulation formats with higher SE more than 1 bit/s/Hz instead of OOK modulation for the system beyond NG-PON2, such as orthogonal frequency-division multiplexing (OFDM), pulse amplitude modulation (PAM), high order QAM. Among these formats, OFDM has gained substantial interests from both the academic and industrial communities by virtue of its substantial advantages like high SE, strong robustness to dispersion and simple distortion equalization [8]–[19]. Moreover, OFDM is transparent to modulation formats and hence easy to upgrade to higher capacity with advanced modulation formats. OFDM-based PON has become one of the most promising solutions for future optical access and data center networks.

Optical OFDM can be mainly classified into direct detection OOFDM (DDO-OFDM) and coherent optical OFDM (CO-OFDM) based on the different detection methods. CO-OFDM has high receiver sensitivity, but the system configuration is complex, which is more suitable for long-haul high-speed optical transmission. The system configuration of DDO-OFDM is fairly simplified and cost-effective, which makes it more suitable for short reach optical communication system.

The high peak-to-average power ratio (PAPR) of the OFDM signal is a severe problem for DDO-OFDM system. High PAPR degrades the performance of OFDM signal, especially for the generation of high order QAM (e.g., 64-, 256- and 1024-QAM) encoded OFDM signals. The OFDM signal with high PAPR requires high-resolution digital-to-analog converters (DACs) and analog-to-digital converters (ADCs), and suffers from the nonlinearity of the electrical and optical components (e.g., RF amplifier, optical modulator and fiber).

The techniques to mitigate PAPR in OFDM system have been studied extensively and several schemes like pre-distortion, coding and probability scheme have been proposed [20]–[22]. However, drawbacks like degrading the performance, reducing spectral efficiency and increasing the complexity also come along with these schemes.

Discrete Fourier transform (DFT)-spread OFDM has been used in wireless communications and has already been incorporated into the uplink of the 4G mobile standard, known as long-term-evolution (LTE) [23]. It has also been introduced into the intensity-modulation/direct-detection (IM/DD) system because of the advantage of PAPR reduction [24]–[27].

In this paper, we compare the performance of DFT-spread OFDM and conventional OFDM in IM/DD system over 40-km standard single mode fiber (SSMF). Compared to conventional OFDM, DFT-spread OFDM has lower PAPR and demonstrates better receiver sensitivity and nonlinearity tolerance performance. It also performs well in resisting nonlinearity distortion from low-bit resolution DAC/ADC. We demonstrated transmission of 11.89 Gbit/s DFT-spread 16-QAM OFDM signal in IM/DD system. Simulation results of Q value and bit error ratio (BER) show that DFT-spread OFDM outperforms conventional OFDM.

The rest of the paper is organized as follows. In Section II, we analyze the operation principle of DFT-Spread OFDM. The simulation setup is described in Section III. Section IV analyzes the simulation results. Finally, the paper is concluded in Section V.

II. OPERATION PRINCIPLE

Fig. 1 shows the DSP processes of DFT-spread OFDM at both transmitter and receiver side. The modulation process is shown in Fig. 1(a). The Original data are first converted into M parallel channels, where M is an integer with the range of $[N/4, N/2-1]$ (N is the IFFT/FFT size), and mapped into M complex QAM symbols. Then M-point DFT is implemented and every mapped symbol can be spread into M subcarriers. To obtain the real-valued outputs from N-point IFFT, Hermitian conjugate symmetric structure is constructed before IFFT. Cyclic prefix (CP) is appended in front of each IFFT output to avoid inter-symbol interference (ISI). The parallel IFFT outputs are then converted into serial data and sent out.

The demodulation process at receiver side is shown in Fig. 1(b). The DSP process mainly includes CP removal, N-point FFT, channel estimation and equalization, M-point

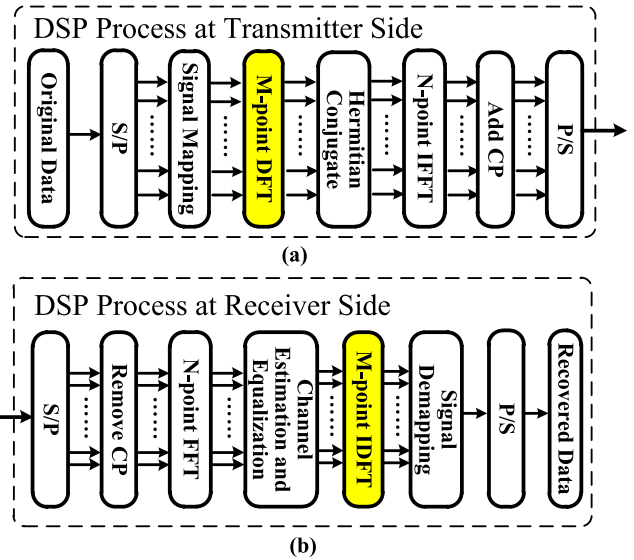


FIGURE 1. The DSP process at (a) transmitter side and (b) receiver side.

IDFT and QAM demapping. It should be noted that except for the DFT and IDFT parts, the other processes are the same as the conventional OFDM. Therefore, upgrading from the existing conventional OFDM to DFT-spread OFDM does not need much modification.

III. SIMULATION SETUP

The simulation setup for the performance investigation of DFT-spread and conventional OFDM signal is shown in Fig. 2. The red, blue and black lines represent the optical, electrical and digital signals respectively. Matlab and VPITransmissionMaker are jointly used for simulation to verify the performance of DFT-Spread OFDM system. Matlab programs are utilized for digital signal generation and demodulation. VPITransmissionMaker is utilized to simulate the electrical and optical modules, as well as the optical fiber links.

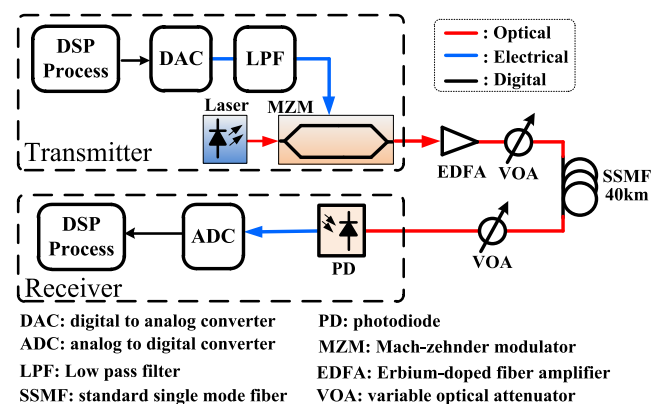


FIGURE 2. Simulation setup for DFT-spread and conventional OFDM.

The Pseudo-Random Binary Sequence (PRBS) is used as the original data. The system sampling rate is set to

be $F_s=10GSa/s$. The OFDM transmitter design allows up to 128 subcarriers. However, not all of the available bandwidth could be used because of the need for oversampling. This is due to the fact that the DAC generates the signal with a zero-order hold characteristic, creating an image (a mirror copy of the baseband) above the Nyquist frequency ($F_s/2$). 99 subcarriers are used to carry data and each data-carrying subcarrier is mapped into 16-QAM. The 99-point DFT outputs are assigned to the corresponding subcarriers. 27 subcarriers in high frequency are empty for oversampling, and the oversampling rate is 1.28. The IFFT size is 256 after Hermitian conjugate symmetric structure constructed. CP with 32 samples is added to avoid ISI. 10 training symbols (TSs) are used every 64 OFDM symbols for channel estimation. An optical OFDM signal with a net data rate of 11.89 Gb/s ($10G \times 4 \times 99/256 \times 256/288 \times 64/74$) is obtained, and the occupied bandwidth is 3.91 GHz ($10G \times (99+1)/128 \times 1/2$). The digital signal after DSP process is loaded to an 8-bit resolution DAC. A low pass filter (LPF) is used to remove the OFDM band image introduced by the DAC. The DAC output is loaded to a Mach-Zehnder modulator (MZM) to generate the modulated optical waveform.

The optical waveform is launched into 40km dispersion uncompensated SSMF. The fiber parameters are set as follows, the dispersion index, attenuation, nonlinear index and effective core area of fiber are 16ps/nm/km, 0.2dB/km, $2.6 \times 10^{-20}m^2/W$ and $80 \times 10^{-12}m^2$ respectively. Erbium-doped fiber amplifier (EDFA) and variable optical attenuator (VOA) are used to control the launch power into fiber.

At the receiver side, another VOA is used to control the received optical power (ROP). The received optical signal is directly detected by a photodiode (PD) and converted to electrical signal. The PD outputs are sampled with an 8-bit resolution ADC and processed with Matlab program for demodulation.

IV. RESULTS AND DISCUSSIONS

We use the simulation system described in section III to evaluate the performance of DFT-spread and conventional OFDM by mean of the indicators like receiver sensitivity, nonlinearity tolerance.

In order to evaluate the system more effectively, in addition to BER, Q-value is also used to evaluate the performance. The definition of Q-value is

$$q = \left(\frac{1}{\sqrt{N \cdot N_{sc}}} \sqrt{\sum_{i=1}^N \sum_{k=1}^{N_{sc}} \frac{|C'_{ik} - C'_{i,ave}|^2}{|C'_{i,ave}|^2}} \right)^{-1}, \quad (1)$$

$$Q = 20 \times \lg(q), \quad (2)$$

where N_{sc} is the number of subcarrier, N is the number of received OFDM symbol, C'_{ik} is the received i -th data symbol on the k -th subcarrier, and $C'_{i,ave}$ is the average of corresponding received OFDM symbols.

Same original data are utilized in both DFT-spread and conventional OFDM modulation. In this simulation research, The PAPR of conventional OFDM signal is 12.9dB, and the PAPR reduced to 10.3dB with the added DFT process. It can be seen that DFT-spread could reduce PAPR effectively.

A. RECEIVER SENSITIVITY ANALYSIS

The receiver sensitivity performance is investigated in this part. The launch power into fiber is fixed at 8dBm. The ROP varies from -10dBm to 0dBm by adjusting the VOA at receiver side.

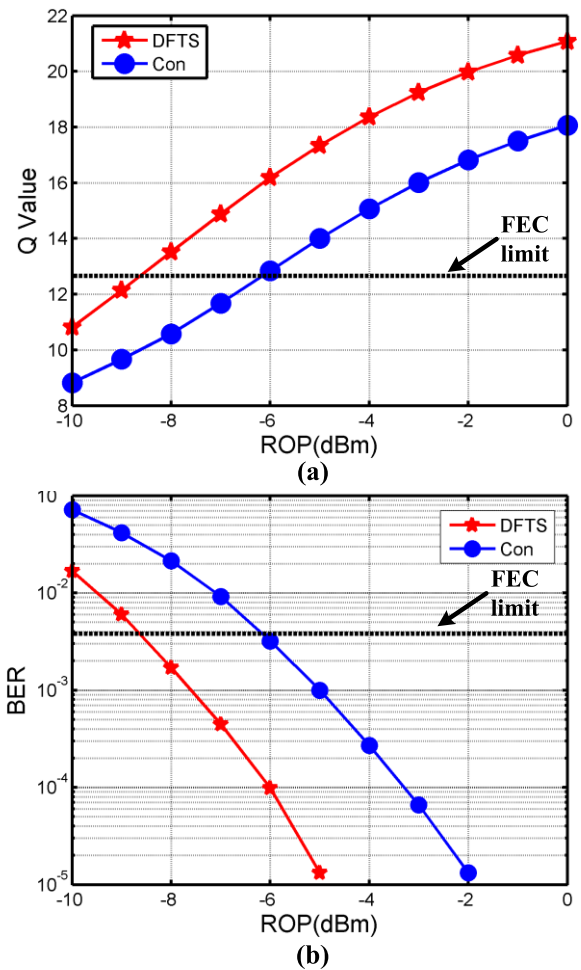


FIGURE 3. (a) Q value and (b) BER performance with different ROP.

Fig. 3 shows the Q value and BER performance with different ROP. The red line represents DFT-Spread OFDM and blue line represents conventional OFDM. The results depicted in Fig. 3 show that the DFT-spread OFDM has better receiver sensitivity performance than conventional OFDM. When the ROP is larger than -5dBm, the DFT-Spread OFDM system is error free, while the ROP should be larger than -2dBm for conventional OFDM to get the error-free status. At the FEC limit, the DFT-Spread OFDM improves the receiver sensitivity about 2.5dB, which means that the DFT-Spread OFDM can be transmitted for a farther distance.

B. NONLINEARITY TOLERANCE ANALYSIS

When the launch power into fiber is too large, the influence of nonlinearity effect will appear and nonlinear distortion will be caused. Since DFT-spread OFDM has lower PAPR, it is expected to have better nonlinearity tolerance. The nonlinearity tolerance performance is investigated in this part. The ROP is fixed at -2dBm. The launch power into fiber varies from 6dBm to 22dBm by adjusting the EDFA and VOA at transmitter side.

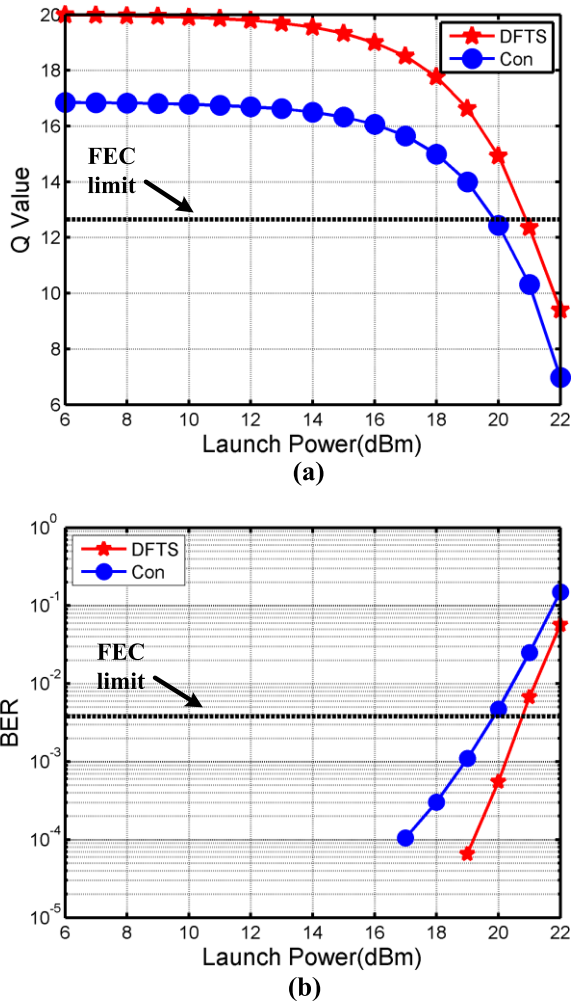
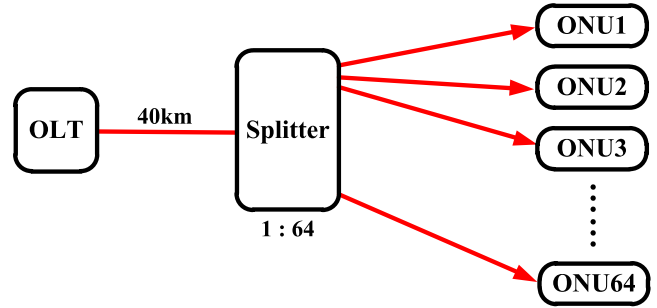


FIGURE 4. (a) Q value and (b) BER performance with different launch power.

Fig. 4 shows the Q value and BER performance with different launch power into fiber. The results depicted in Fig. 4 show that the performance of DFT-spread OFDM is always better than that of conventional OFDM, 3dB Q value gain could be obtained at low launch power. The system performance begins to deteriorate obviously when the launch power reaches 14dBm. When the launch power is larger than 17dBm, the errors appear for the conventional OFDM system, while for DFT-Spread OFDM errors appear until launch power is larger than 19dBm. The DFT-Spread OFDM appears better nonlinearity tolerance performance than conventional OFDM. At the FEC limit, the DFT-Spread



OLT: Optical Line Terminal
ONU: Optical Network Unit

FIGURE 5. PON downstream setup.

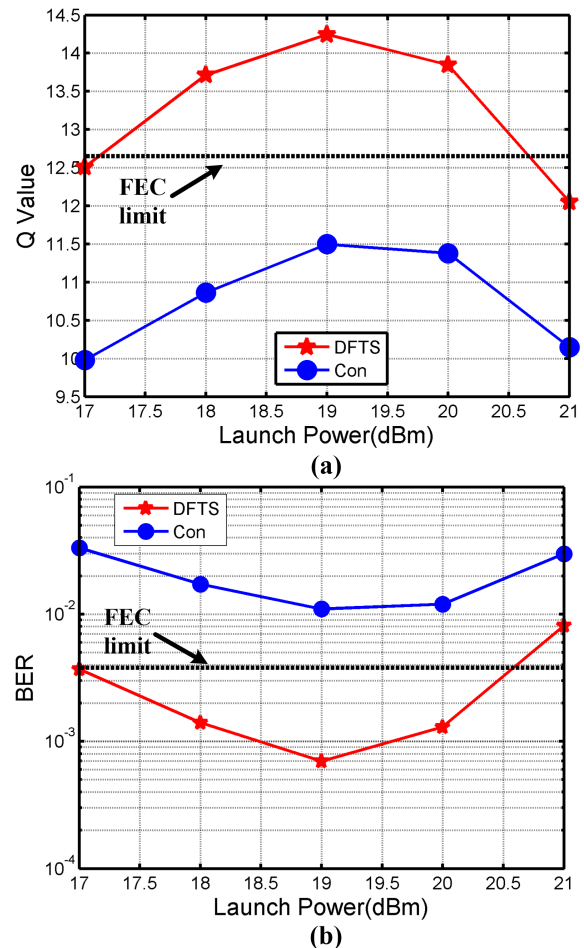


FIGURE 6. PON downstream performance.

OFDM improves the nonlinearity tolerance about 1dB. The results above prove that DFT-spread has better nonlinearity tolerance and larger acceptable launch power than conventional OFDM.

C. PON DOWNSTREAM SETUP

The NG-PON2 systems require flexibility to balance trade-offs in speed, distance, and split ratios for

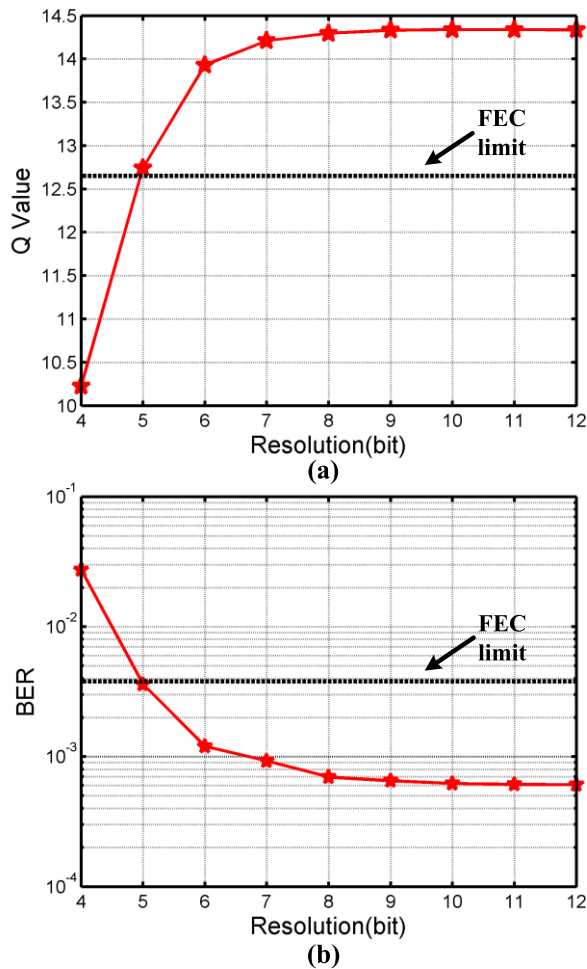


FIGURE 7. (a) Q value and (b) BER performance with different resolution.

various applications. For the downstream channel, this parameter combinations should be met, 40 Gbit/s downstream capacity and 20 km reach with at least 1:64 split. Since TWDM is adopted for NG-PON2, the single wavelength transmission rate is 10 Gbit/s.

In this paper, we consider the PON downstream setup as shown in Fig.5. The fiber link is 40 km, and the split ratio is 1:64. The single wavelength net data rate is 11.89Gb/s as described in section III.

The simulation setup is adjusted for the PON downstream study. The 1:64 splitter is equivalent to 18dB power attenuation, so the VOA at the receiver side is fixed at 18dB for simplicity. Consider both receiver sensitivity and nonlinearity tolerance performance shown above, the launch power into fiber varies from 17dBm to 21dBm. The other parameters are the same as previous simulation. Both DFT-spread and conventional OFDM performance are investigated in the PON downstream system.

Fig. 6 shows simulation results. The system performance is influenced by both noise and nonlinearity. The results show that the DFT-Spread OFDM could meet the requirement of FEC limit with launch power from 18dBm to 20dBm, while for the conventional OFDM, the FEC requirement is unable

to be met anymore. The results mean that the DFT-Spread OFDM is suitable for the assumed PON downstream system in Fig. 5, while the conventional OFDM could not meet the requirement.

D. DAC/ADC RESOLUTION ANALYSIS

For practical system, the bit resolution of DAC and ADC should be considered. Low bit resolution will cause signal nonlinearity distortion and deteriorate system performance. And high bit resolution will increase the computational complexity and system cost. Therefore, an appropriate bit resolution is needed to be utilized by considering both facts. We adjusted the bit resolution of DAC/ADC and investigate the system performance in this part.

Fig. 7 shows the Q value and BER performance with different bit resolution. The launch power and ROP are fixed at 19dBm and -7dBm respectively. The resolution varies from 4-bit to 12-bit. The results show that the FEC limit requirement could be met when bit resolution higher than 5-bit, which means that DFT-spread OFDM performs well in resisting nonlinearity distortion caused by DAC/ADC. When the resolution achieves 8-bit, the system performs well. As the resolution continues to increase, system performance does not improve significantly. Therefore, we believe that the 8-bit resolution is the most reasonable choice for the practical system.

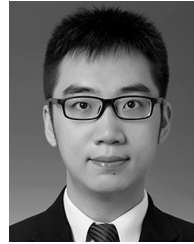
V. CONCLUSION

In this paper, we investigated the performance of DFT-spread 16-QAM OFDM signal in an IM/DD system. We find that DFT-spread OFDM could reduce the PAPR effectively, and hence improve the nonlinearity tolerance. Furthermore, DFT-spread OFDM improves the receiver sensitivity and also represents good robustness to low-resolution nonlinearity distortion of DAC/ADC. The measured BER of DFT-spread OFDM signal after 40-km SSMF is well less than the FEC limit of 3.8×10^{-3} . Moreover, The DFT-spread OFDM performs well in the assumed PON downstream system where conventional OFDM could not meet the requirement. The research results show that DFT-spread OFDM is suitable for the high-speed short reach optical communication systems, and DFT-spread OFDM-PON is a promising candidate for the system beyond NG-PON2.

REFERENCES

- [1] M. Mazur, A. Lorences-Riesgo, J. Schröder, P. A. Andrekson, and M. Karlsson, "10 Tb/s PM-64QAM self-homodyne comb-based super-channel transmission with 4% shared pilot tone overhead," *J. Lightw. Technol.*, vol. 36, no. 16, pp. 3176–3184, Aug. 2018.
- [2] Z. Yang et al., "Radial basis function neural network enabled C-band 4×50 Gb/s PAM-4 transmission over 80 km SSMF," *Opt. Lett.*, vol. 43, no. 15, pp. 3542–3545, Aug. 2018.
- [3] M. Xiang, Z. Xing, E. El-Fiky, M. Morsy-Osman, Q. Zhuge, and D. V. Plant, "Single-lane 145 Gbit/s IM/DD transmission with faster-than-Nyquist PAM4 signaling," *IEEE Photon. Technol. Lett.*, vol. 30, no. 13, pp. 1238–1241, Jul. 1, 2018.
- [4] K.-H. Mun, S.-M. Kang, and S.-K. Han, "Multiple-noise-tolerant CO-OFDMA-PON uplink multiple access using AM-DAPSK-OFDM with reflective ONUs," *J. Lightw. Technol.*, vol. 36, no. 23, pp. 5462–5469, Dec. 2018.

- [5] J. Li *et al.*, "Real-time bidirectional coherent ultra-dense TWDM-PON for 1000 ONUs," *Opt. Express*, vol. 26, no. 18, pp. 22976–22984, Sep. 2018.
- [6] X. Tang *et al.*, "Equalization scheme of C-band PAM4 signal for optical amplified 50-Gb/s PON," *Opt. Express*, vol. 26, no. 25, pp. 33418–33427, Dec. 2018.
- [7] Y. Luo *et al.*, "Time- and wavelength-division multiplexed passive optical network (TWDM-PON) for next-generation PON stage 2 (NG-PON2)," *J. Lightw. Technol.*, vol. 31, no. 4, pp. 587–593, Feb. 15, 2013.
- [8] J. Armstrong, "OFDM for optical communications," *J. Lightw. Technol.*, vol. 27, no. 3, pp. 189–204, Feb. 1, 2009.
- [9] E. Giacomidis *et al.*, "Comparison of DSP-based nonlinear equalizers for intra-channel nonlinearity compensation in coherent optical OFDM," *Opt. Lett.*, vol. 41, no. 11, pp. 2509–2512, Jun. 2016.
- [10] X. Du, J. Zhang, Y. Li, C. Yu, and P.-Y. Kam, "Efficient joint timing and frequency synchronization algorithm for coherent optical OFDM systems," *Opt. Express*, vol. 24, no. 17, pp. 19969–19977, Aug. 2016.
- [11] R. Giddings, "Real-time digital signal processing for optical OFDM-based future optical access networks," *J. Lightw. Technol.*, vol. 32, no. 4, pp. 553–570, Feb. 15, 2014.
- [12] M. Chen, G. Liu, H. Zhou, Q. Chen, and J. He, "Inter-symbol differential detection-enabled sampling frequency offset compensation for DDO-OFDM," *IEEE Photon. Technol. Lett.*, vol. 30, no. 24, pp. 2095–2098, Dec. 15, 2018.
- [13] M. Chen, J. He, Q. Fan, Z. Dong, and L. Chen, "Experimental demonstration of real-time high-level QAM-encoded direct-detection optical OFDM systems," *J. Lightw. Technol.*, vol. 33, no. 22, pp. 4632–4639, Nov. 15, 2015.
- [14] C. Ju, N. Liu, X. Chen, and Z. Zhang, "SSBI mitigation in A-RF-tone-based VSSB-OFDM system with a frequency-domain Volterra series equalizer," *J. Lightw. Technol.*, vol. 33, no. 23, pp. 4997–5006, Dec. 2015.
- [15] X. Yi, W. Shieh, and Y. Ma, "Phase noise effects on high spectral efficiency coherent optical OFDM transmission," *J. Lightw. Technol.*, vol. 26, no. 10, pp. 1309–1316, May 15, 2008.
- [16] H. Zhou *et al.*, "Joint timing and frequency synchronization based on FrFT encoded training symbol for coherent optical OFDM systems," in *Proc. OFC*, Mar. 2016, pp. 1–3, Paper. Tu3K.6.
- [17] Y. Li and D. Ding, "Investigation into constant envelope orthogonal frequency division multiplexing for polarization-division multiplexing coherent optical communication," *Opt. Eng.*, vol. 56, no. 9, 2017, Art. no. 096108.
- [18] Y. Li and D. Ding, "Constant envelope OFDM scheme for 6PolSK-QPSK," *Opt. Commun.*, vol. 410, pp. 841–845, Mar. 2018.
- [19] Y. Li and D. Ding, "Spectrum efficiency improvement for quasi-constant envelope OFDM," *IEEE Photon. Technol. Lett.*, vol. 30, no. 15, pp. 1392–1395, Aug. 1, 2018.
- [20] J. Armstrong, "Peak-to-average power reduction for OFDM by repeated clipping and frequency domain filtering," *Electron. Lett.*, vol. 38, no. 5, pp. 246–247, Feb. 2002.
- [21] J. A. Davis and J. Jedwab, "Peak-to-mean power control and error correction for OFDM transmission using Golay sequences and Reed-Müller codes," *Electron. Lett.*, vol. 33, no. 4, pp. 267–268, Feb. 1997.
- [22] J. Wang, Y. Guo, and X. Zhou, "PTS-clipping method to reduce the PAPR in ROF-OFDM system," *IEEE Trans. Consum. Electron.*, vol. 55, no. 2, pp. 356–359, May 2009.
- [23] H. G. Myung, J. Lim, and D. J. Goodman, "Peak-to-average power ratio of single carrier FDMA signals with pulse shaping," in *Proc. IEEE 17th Int. Symp. Pers., Indoor Mobile Radio Commun.*, Sep. 2006, pp. 1–5.
- [24] F. Li, X. Li, J. Zhang, and J. Yu, "Transmission of 100-Gb/s VSB DFT-spread DMT signal in short-reach optical communication systems," *IEEE Photon. J.*, vol. 7, no. 5, Oct. 2015, Art. no. 7904307.
- [25] Y. Tang, W. Shieh, and B. S. Krongold, "DFT-spread OFDM for fiber nonlinearity mitigation," *IEEE Photon. Technol. Lett.*, vol. 22, no. 16, pp. 1250–1253, Aug. 15, 2010.
- [26] M. Chen *et al.*, "Experimental demonstration of an IFFT/FFT size efficient DFT-spread OFDM for short reach optical transmission systems," *J. Lightw. Technol.*, vol. 34, no. 9, pp. 2100–2105, May 2016.
- [27] S. Karabetos, E. Pikasis, T. Nikas, A. Nassiopoulos, and D. Syvridis, "DFT-spread DMT modulation for 1-Gb/s transmission rate over 100 m of 1-mm SI-POF," *IEEE Photon. Technol. Lett.*, vol. 24, no. 10, pp. 836–838, May 15, 2012.



YUPENG LI received the Ph.D. degree in communication and information system from the Beijing University of Posts and Telecommunications, Beijing, China, in 2015. Since 2015, he has been a Lecturer with the Tianjin Key Laboratory of Wireless Mobile Communications and Power Transmission, Tianjin Normal University, Tianjin, China. His current research interests include advanced modulation schemes, optical access networks, and coherent optical communication systems.



JIawei HAN received the Ph.D. degree in electrical engineering from the Beijing University of Posts and Telecommunications, Beijing, China, in 2013. In 2015, he joined the Tianjin Key Laboratory of Wireless Mobile Communications and Power Transmission, Tianjin Normal University. Since then, he has been involved in research on MIMO technologies in fiber-optic communication systems.



XIAONAN ZHAO received the Ph.D. degree from Tianjin University, Tianjin, China, in 2015. He is currently with the Tianjin Key Laboratory of Wireless Mobile Communications and Power Transmission, Tianjin Normal University, Tianjin. His research interest includes wireless communication channel measurement and modeling.

• • •